remote sensing

MDPI

Article

Estimating the Fractional Vegetation Cover from GLASS Leaf Area Index Product

Zhiqiang Xiao [1,*], Tongtong Wang [1], Shunlin Liang [1,2] and Rui Sun [1]

[1] State Key Laboratory of Remote Sensing Science, School of Geography, Beijing Normal University, Beijing 100875, China; tdzyglwtt@163.com (T.W.); sunrui@bnu.edu.cn (R.S.)

[2] Department of Geographical Sciences, University of Maryland, College Park, MD 20742, USA; sliang@umd.edu

* Correspondence: zhqxiao@bnu.edu.cn; Tel.: +86-10-5880-7698; Fax: +86-10-5880-5274

Academic Editors: Parth Sarathi Roy and Prasad S. Thenkabail
Received: 28 December 2015; Accepted: 13 April 2016; Published: 16 April 2016

Abstract: The fractional vegetation cover (FCover) is an essential biophysical variable and plays a critical role in the carbon cycle studies. Existing FCover products from satellite observations are spatially incomplete and temporally discontinuous, and also inaccurate for some vegetation types to meet the requirements of various applications. In this study, an operational method is proposed to calculate high-quality, accurate FCover from the Global LAnd Surface Satellite (GLASS) leaf area index (LAI) product to ensure physical consistency between LAI and FCover retrievals. As a result, a global FCover product (denoted by TRAGL) were generated from the GLASS LAI product from 2000 to present. With no missing values, the TRAGL FCover product is spatially complete. A comparison of the TRAGL FCover product with the Geoland2/BioPar version 1 (GEOV1) FCover product indicates that these FCover products exhibit similar spatial distribution pattern. However, there were relatively large discrepancies between these FCover products over equatorial rainforests, broadleaf crops in East-central United States, and needleleaf forests in Europe and Siberia. Temporal consistency analysis indicates that TRAGL FCover product has continuous trajectories. Direct validation with ground-based FCover estimates demonstrated that TRAGL FCover values were more accurate (RMSE = 0.0865, and R^2 = 0.8848) than GEOV1 (RMSE = 0.1541, and R^2 = 0.7621).

Keywords: FCover; LAI; validation; GLASS; GEOV1

1. Introduction

The fractional vegetation cover (FCover), defined as the fraction of green vegetation as seen from the nadir of the total statistical area, is a canopy-intrinsic variable that depends only on the canopy structural attributes and plays a critical role in climate and hydrologic modeling, natural hazards monitoring, and soil erosion risk assessment [1,2]. Satellite observations provide the only feasible way to estimate FCover at regional and global scales.

Many algorithms have been developed to retrieve FCover from satellite remote sensing data [3–5] and multiple global FCover products have been generated from data acquired by the Advanced Very High Resolution Radiometer (AVHRR) [1], the Polarization and Directionality of Earth Reflectance (POLDER) instrument aboard the Japanese space-borne ADEOS-I [6], and SPOT/VEGETATION [3,7]. In general, three types of algorithms are employed, empirical methods, spectral mixture analysis (SMA) methods and physical methods. Empirical methods are based on statistical relationships between FCover and vegetation indices or specific spectral reflectance to retrieve FCover from remote sensing data. They are calibrated for distinct vegetation types using field measurements and concurrently acquired satellite images [8–12]. The empirical methods are computationally efficient in operating with large amounts of data and widely used in FCover estimation on a regional scale. The limitation of

relationship based approaches is that the resulting formulas are influenced by vegetation type and soil background. SMA methods estimate FCover at a sub-pixel level based on endmembers from remote sensing data [1,13,14]. These methods assume that the pixel composite spectral responses are the linear sum of the reflectance measurements of the individual endmembers, weighted by their relative proportions [15]. The endmembers can be either developed from laboratory or field spectra or derived directly from remote sensing data. These SMA methods, especially the pixel dimidiate model, were widely used to estimate FCover and achieved good results at the regional scale [16]. However, it is difficult to determine the endmembers and the spectral of the endmembers at the global scale for FCover estimation because the land surface is complex and the spectral characteristics of objects are varied. Physical methods are based on the inversion of canopy radiative transfer models describing the transfer of solar radiation in vegetation canopies. Since the physical methods can be adjusted for a wide range of situations [17], radiative transfer models are increasingly used in the inverse mode to estimate FCover from remotely-sensed data. However, inversion techniques based on iterative minimization of a cost function require hundreds of runs of the canopy radiative transfer model for each pixel; therefore, they are computationally too demanding [17]. For operational applications, artificial neural networks (ANNs) are popular inversion techniques that are based on a pre-computed reflectance database [18].

Nevertheless, currently available empirical, SMA, and physical methods generally use only single-phase remote-sensing data to retrieve FCover values. A consequence of using limited information during the inversion process is that the FCover products generated by these methods are spatially incomplete and temporally discontinuous, and also insufficiently accurate to meet the requirements of various applications [19]. Camacho *et al.* evaluated the performance of the GEOV1 FCover product and demonstrated that the GEOV1 FCover product presented the higher percentage of missing values at high latitudes in the northern hemisphere, with a wide variability as a function of the period of the year, mainly due to snow coverage changes along the year as well as increase in observations under dark conditions, particularly above the polar circle in winter, and the equatorial region also presents a large fraction of gaps (up to 50%) as a consequence of the higher cloudiness [19]. The RMSE of the GEOV1 FCover product is around 0.1. It is still unable to meet the threshold accuracy requirements ($\pm$0.05). The low accuracy and poor quality, in many cases, among existing FCover products require improvements or new products. Furthermore, currently available inversion methods are generally parameter-specific algorithms to separately retrieve land surface parameters from satellite observations, which results in a lack of physical consistency between current land surface parameter products [20,21].

To improve the quality and accuracy of satellite products, the Global LAnd Surface Satellite (GLASS) product suite was developed, and the phase I products include leaf area index (LAI), shortwave broadband albedo, longwave broadband emissivity, downwelling shortwave radiation, and photosynthetically active radiation (PAR) [22,23]. Efforts are being made to generate seven additional products, including the fraction of absorbed photosynthetically active radiation (FAPAR), FCover, gross primary production (GPP), Evaportranspiration (ET), net radiation, net longwave radiations, and land surface temperature (LST). The GLASS LAI product was retrieved from time-series MODIS and Advanced Very High Resolution Radiometer (AVHRR) surface reflectance data [24]. Extensive validations for all biome types demonstrate that the GLASS LAI product provides temporally-continuous LAI profiles with much improved quality and accuracy compared to the current MODIS and GEOV1 LAI products [25].

This paper aims to develop an operational method to generate a high-quality global FCover product from the GLASS LAI data to ensure physical consistency between LAI and FCover retrievals. The method was applied to generate a global FCover product (spanning from 2000 to 2014) from the GLASS LAI data derived from MODIS surface reflectance data. The spatial and temporal consistencies of the retrieved FCover values in this study are evaluated by comparison with GEOV1 FCover values, and the accuracy of the retrieved FCover values was validated against ground-based FCover estimates.

2. Data

2.1. Satellite Data Sets

The GLASS LAI product was used to derive FCover product, and GEOV1 FCover product was compared with the FCover product proposed in this study. The main characteristics of the GLASS LAI product and the GEOV1 FCover product are described below.

2.1.1. GLASS LAI Product

The GLASS LAI product is one of the longest duration LAI products in the world. It has a temporal resolution of 8 days and spans 1981–2014. For the period 1981–1999, AVHRR reflectance data from NASA's Land Long-Term Data Record (LTDR) project [26] were used to retrieve the LAI product, which was provided in a geographic latitude/longitude projection at spatial resolution of 0.05° (~5 km at the Equator). For the period 2000–2014, the LAI product was derived from MODIS surface reflectance data and provided in a sinusoidal projection at spatial resolution of 1 km [25]. The GLASS LAI product was retrieved using general regression neural networks (GRNNs). Unlike existing neural network methods that use remote sensing data acquired only at a specific time to retrieve LAI, the GRNNs were trained using fused time series LAI values from MODIS and CYCLOPES LAI products and reprocessed time series MODIS/AVHRR reflectance. The reprocessed MODIS/AVHRR reflectance values from an entire year were input to the GRNNs to estimate the one-year LAI profiles. The GLASS LAI product was generated and released by the Center for Global Change Data Processing and Analysis of Beijing Normal University [27]. It is also available from the Global Land Cover Facility [28].

2.1.2. GEOV1 FCover Product

The GEOV1 FCover product has been available since 1999 from the Copernicus Land Monitoring Services [29]. The product is provided in a Plate Carrée projection at 1/112° spatial resolution and a 10-day frequency. The GEOV1 FCover product was derived from SPOT/VEGETATION sensor data using back-propagation neural networks. The CYCLOPES FCover product was scaled to train the back-propagation neural networks with the SPOT/VEGETATION top-of-canopy directionally-normalized reflectance values over the BELMANIP (Benchmark Land Multisite Analysis and Intercomparison of Products) network of sites [7]. The calibrated neural networks were used to generate the GEOV1 FCover product from SPOT/VEGETATION top-of-canopy directionally-normalized reflectance data.

2.2. Field Measured Data

FCover ground measurements are from the Validation of Land European Remote sensing Instrument (VALERI) project [30]. The FCover ground measurements were calculated from digital hemispherical photos using the CAN_EYE software package [31]. For the assessment and validation of the moderate-resolution FCover products, ground "point" measurements are not suitable for making direct comparisons with moderate-resolution pixels due to the surface heterogeneity. According to guidelines defined by the CEOS/WGCV LPV subgroup, an empirical transfer function between high-resolution reflectance data and the FCover ground measurements for a site was established to derive a high-resolution FCover map that was then aggregated to the moderate-resolution products for comparison [32]. Forty-seven high-resolution FCover maps over 28 sites from the VALERI project [30] were collected to validate the accuracy of the FCover product proposed in this study and the GEOV1 FCover product. The characteristics of the validation sites and associated mean values and standard deviations of the high-resolution FCover maps over 3 km × 3 km regions centered on the location of the sites are shown in Table 1, and they were also reported in Camacho *et al.* [19].

Table 1. Characteristics of the 28 validation sites.

Site Name	Lat (°)	Lon (°)	Biome Type	Year	DOY	Mean FCover	Uncertainties of FCover
Alpilles2	43.8103	4.7146	Broadleaf crops	2002	204	0.349	0.264
Barrax	39.0569	−2.1041	Broadleaf crops	2003	193	0.236	0.294
Cameron	−32.5983	116.2542	Broadleaf forests	2004	63	0.414	0.079
Chilbolton	51.1640	−1.4306	Broadleaf crops	2006	166	0.647	0.192
Counami	5.3471	−53.2377	Broadleaf forests	2001	269	0.838	0.030
				2002	286	0.858	0.003
Demmin	53.8921	13.2071	Broadleaf crops	2004	164	0.586	0.215
Donga	9.7701	1.7783	Grasses and cereal crops	2005	172	0.423	0.161
Fundulea	44.4061	26.5830	Broadleaf crops	2001	128	0.341	0.203
				2002	144	0.374	0.263
				2003	144	0.319	0.192
Gilching	48.0818	11.3204	Broadleaf crops	2002	199	0.676	0.214
Gnangara	−31.5338	115.8823	Broadleaf forests	2004	61	0.221	0.035
Gourma	15.3247	−1.5546	Grasses and cereal crops	2000	244	0.236	
				2001	275	0.126	
Haouz	31.6592	−7.6002	Broadleaf crops	2003	71	0.248	0.182
Hirsikangas	62.6438	27.0114	Needleleaf forests	2003	226	0.644	0.201
				2004	190	0.537	0.234
				2005	159	0.442	0.210
Hombori	15.3309	−1.4750	Savannah	2002	242	0.2	
Hyytiälä	61.8513	24.3076	Needleleaf forests	2008	188	0.461	0.223
Jarvselja	58.2987	27.2622	Needleleaf forests	2000	188	0.705	0.169
				2001	165	0.783	0.141
				2002	178	0.793	0.108
				2003	208	0.803	0.142
				2005	180	0.842	0.118
				2007	112	0.535	0.295
				2007	199	0.731	0.189
Laprida	−36.9904	−60.5526	Grasses and cereal crops	2001	311	0.722	0.117
				2002	292	0.534	0.049
Larose	45.3804	−75.2170	Needleleaf forests	2003	219	0.847	0.156
Larzac	43.9375	3.1229	Grasses and cereal crops	2002	183	0.3	0.065
Nezer	44.5679	−1.0382	Needleleaf forests	2000	211	0.499	0.149
				2001	99	0.363	0.193
				2001	175	0.785	0.194
				2002	107	0.304	0.136
Plan-de-Dieu	44.1986	4.9481	Broadleaf crops	2004	189	0.172	0.130
Puéchabon	43.7245	3.6519	Broadleaf forest	2001	164	0.54	0.157
Rovaniemi	66.4556	25.3514	Needleleaf forests	2004	161	0.423	0.137
				2005	166	0.497	0.182
Sonian	50.7681	4.4110	Needleleaf forests	2004	174	0.903	0.028
Sud_Ouest	43.5062	1.2375	Broadleaf crops	2002	189	0.352	0.219
Turco	−18.2350	−68.1836	Shrubs	2001	208	0.106	0.026
				2002	240	0.02	0.013
				2003	105	0.044	0.011
Wankama	13.6449	2.6353	Savannah	2005	174	0.036	0.035
Zhang_Bei	41.2787	114.6877	Grasses and cereal crops	2002	221	0.353	0.143

3. Methodology

3.1. Calculation of FCover

In this study, the estimation of FCover is based on the measures of the transmittance of light through the canopy considering the vegetation elements as opaque. As light passes downward through the top of a canopy, the fraction of the light transmitted through the canopy can be approximated using an exponential model [33]:

$$P_{\mathrm{tr}}(\varphi) = e^{-\sqrt{a}\times k_c(\varphi)\times\Omega\times lai} \quad (1)$$

where lai is the leaf area index of the canopy, Ω is the clumping index taking into account the non-random spatial distribution of phyto-elements within the canopy, a is the absorptivity of leaves for radiation, φ is the solar zenith angle, and $k_c(\varphi)$ is the canopy extinction coefficient. For an ellipsoidal leaf angle distribution, $k_c(\varphi)$ is calculated as follows:

$$k_c(\varphi) = \frac{\sqrt{x^2 + \tan^2(\varphi)}}{x + 1.774 \times (x + 1.182)^{-0.733}} \quad (2)$$

where x is the ratio of average projected areas of canopy elements on horizontal and vertical surfaces. Different values are assigned to x for different vegetation types. x is set to 0.8 for grasses and crops, 1.0 for shrubs and savannah, and 1.2 for forest [33]. FCover corresponds to the complement to unity of the transmittance of light in the nadir viewing direction:

$$fCover = 1 - P_{tr}(0) \quad (3)$$

To quantify the importance of the input parameters for Equation (3) on FCover and characterize their effects, a sensitivity analysis of FCover to target composition and architecture was performed using the extended Fourier amplitude sensitivity test (EFAST) originally developed by Cukier *et al.* [34,35] and extended by Saltelli *et al.* [36]. EFAST is a variance based method and has proven one of the most reliable methods among these techniques [37], although computationally expensive [38]. It provides a first-order and a total-order sensitivity index for each input parameter. The first-order sensitivity index expresses the additive effect of the corresponding input parameter, whereas the total-order sensitivity index is the overall measure of importance and incorporates the interactions of the input parameters.

Various ranges of input parameters used to calculate FCover are shown in Table 2. An input sample of 49,995 combinations of input parameters was provided by EFAST and used to calculate 49,995 FCover values using Equation (3). Sensitivity analysis was performed on this set of FCover values (Figure 1). The first-order and total-order indices of sensitivity analysis demonstrate that LAI is the only sensitive parameter. Therefore, FCover values calculated from Equation (3) are primarily influenced by LAI of the vegetation canopy.

For the above scheme, the GLASS LAI product and the clumping index map derived by He *et al.* [39] was used to calculate the FCover values in this study. The clumping index map has a spatial resolution of 500 m and was aggregated to 1 km resolution to maintain a spatial resolution consistent with the GLASS LAI product using a simple spatial averaging method.

Table 2. Range of input parameters for Equation (3).

Factors	Unit	Range of Variation	Distribution
Leaf area index	m^2/m^2	[0, 8]	uniform
Clumping index	–	[0.5, 1.0]	uniform
Solar zenith angle	Degrees	0.0	–
Absorptivity of leaves	–	1.0	–
Ratio of average projected areas of canopy elements on horizontal and vertical surfaces	–	[0.5, 2.0]	uniform

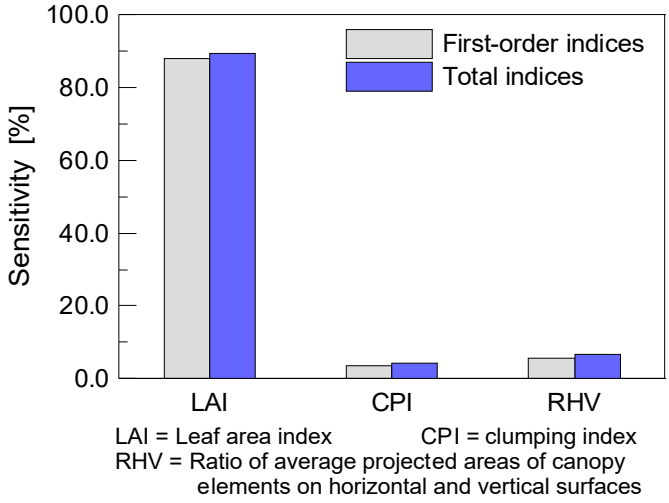

Figure 1. First-order and total-order indices of sensitivity analysis for Equation (3).

3.2. Comparison and Analysis

For clarification, the FCover product derived in this study is denoted by TRAGL. Just like the GLASS LAI product, the TRAGL FCover product has 8-day temporal and 1 km spatial resolution and is provided in a sinusoidal projection from 2000 to 2014. The spatial and temporal consistencies of the TRAGL FCover product are assessed by comparison with the GEOV1 FCover product, and the accuracy of the TRAGL FCover values was evaluated against ground-based FCover estimates.

For comparisons of spatial consistency, the TRAGL and GEOV1 FCover products were re-projected onto the geographic latitude/longitude projection using nearest-neighbor resampling and were aggregated to 0.05° resolution using spatial averaging for the sake of computation efficiency. The average value over a 0.05° pixel was computed if more than 70% of the pixels projected into the 0.05° pixel had FCover values. The FCover products were then aggregated into a monthly time step by computing the monthly average from the FCover values. The global maps of mean FCover for the TRAGL and GEOV1 FCover products from 2001 to 2005 in January and July were computed to investigate spatial patterns specific to a given product as well to check the fraction and distribution in space of the missing data. Histograms of the TRAGL and GEOV1 FCover products from 2001 to 2005 were generated for each biome type according to the MODIS land-cover type product (MCD12Q1) to analyze the similarities and differences between these FCover products. To further evaluate the consistency between the TRAGL and GEOV1 FCover products, the differences between these FCover products from 2001 to 2005 were computed as a function of latitude and as a function of the biome type to qualitatively assess the main discrepancies between these FCover products.

Temporal consistency between TRAGL and GEOV1 FCover products was evaluated over a sample of VALERI sites with different biome classes. Detailed information about the sites and mean values and standard deviations of the high resolution FCover maps over the 3 km × 3 km regions centered on the location of the sites are given in Table 1. For comparison of temporal consistency, the original temporal resolution for each FCover product was considered. Average FCover profiles for the TRAGL and GEOV1 FCover products over 3 × 3 pixels centered on the selected sites were calculated to reduce effects from co-registration errors between them. The average FCover value over the 3 × 3 pixels was computed if there were more than five FCover values among the nine pixels [19]. The average FCover profiles over one year were compared for each site to provide a qualitative assessment of seasonal variations between the products. The specific years used for comparison were not the same for all sites, but varied according to the availability of the high resolution FCover maps derived from ground measurements.

The TRAGL and GEOV1 FCover products were compared with high-resolution FCover maps to evaluate differences in FCover magnitude between the products. The high-resolution FCover maps and the TRAGL and GEOV1 FCover products were aggregated over 3 km $\times$ 3 km regions centered on the location of the validation sites using spatial averaging. TRAGL and GEOV1 FCover values were linearly interpolated to the acquisition date of FCover ground measurements if the two closest FCover values were within $\pm$10 days from that date. A total of 28 sites, providing 47 high resolution FCover maps were retained for which TRAGL or GEOV1 FCover products provided FCover values.

4. Result Analysis

4.1. Comparison with GEOV1 FCover Product

4.1.1. Spatial Consistency

Figure 2 show the global maps of the mean values for the TRAGL and GEOV1 FCover products for January and July 2001−2005. Areas masked in dark gray correspond to pixels where the FCover values are zero, and areas masked in light gray correspond to pixels where the FCover values are missing. GEOV1 FCover product has many missing pixels in rainforest regions and in mid- and high-latitude zones of the northern hemisphere, especially in January. Camacho *et al.* [19] reported that the GEOV1 products presented the higher percentage of missing values at high latitudes in the northern hemisphere, with a wide variability as a function of the period of the year (it maximize in winter time), mainly due to snow coverage changes along the year as well as increase in observations under dark conditions particularly above the polar circle in winter, and also presented a large fraction of gaps (up to 50%) over the equatorial region as a consequence of the higher cloudiness. However, there are no missing data for the TRAGL FCover product, because the retrieval algorithm uses the spatially and temporally complete GLASS LAI product.

The TRAGL and GEOV1 FCover products are generally consistent in their spatial patterns. Higher FCover values are produced over equatorial forest regions and around 50°N−60°N, whereas they are intermediate at mid- and high-latitude zones, and very low over sparsely vegetated areas. However, discrepancies are evident in the relative magnitude of the FCover products. In January, TRAGL FCover values are between 0.05 and 0.15 lower than those of GEOV1 for tropical rainforests in Amazon River Basin and Southeast Asia. At these regions, the GEOV1 FCover values can reach 0.99. However, the GEOV1 FCover values are significantly lower than the TRAGL FCover values over the Congo Basin and the Gulf of Guinea. The largest difference between the TRAGL and GEOV1 FCover values at these regions goes up to 0.4. In July, GEOV1 FCover values are slightly lower than those of TRAGL in Amazon rainforest region, but clearly higher than those of TRAGL over broadleaf crops in East-central United States and needleleaf forests in Europe and Siberia. The GEOV1 FCover algorithm proposed to correct for the systematic underestimation of CYCLOPES FCover product by applying a scaling factor. These discrepancies between the TRAGL and GEOV1 FCover products should be partly explained by a slightly too large scaling factor, resulting in more dynamic FCover values. These discrepancies should probably also be explained by a lack of representativeness of the training data base used to calibrate the algorithm [19]. Compared with the GEOV1 FCover product, the TRAGL FCover product reports a more uniform signal. The TRAGL FCover values for tropical rainforests present almost no seasonality, as expected for these evergreen forests, which is consistent with the findings of Camacho *et al.* [19].

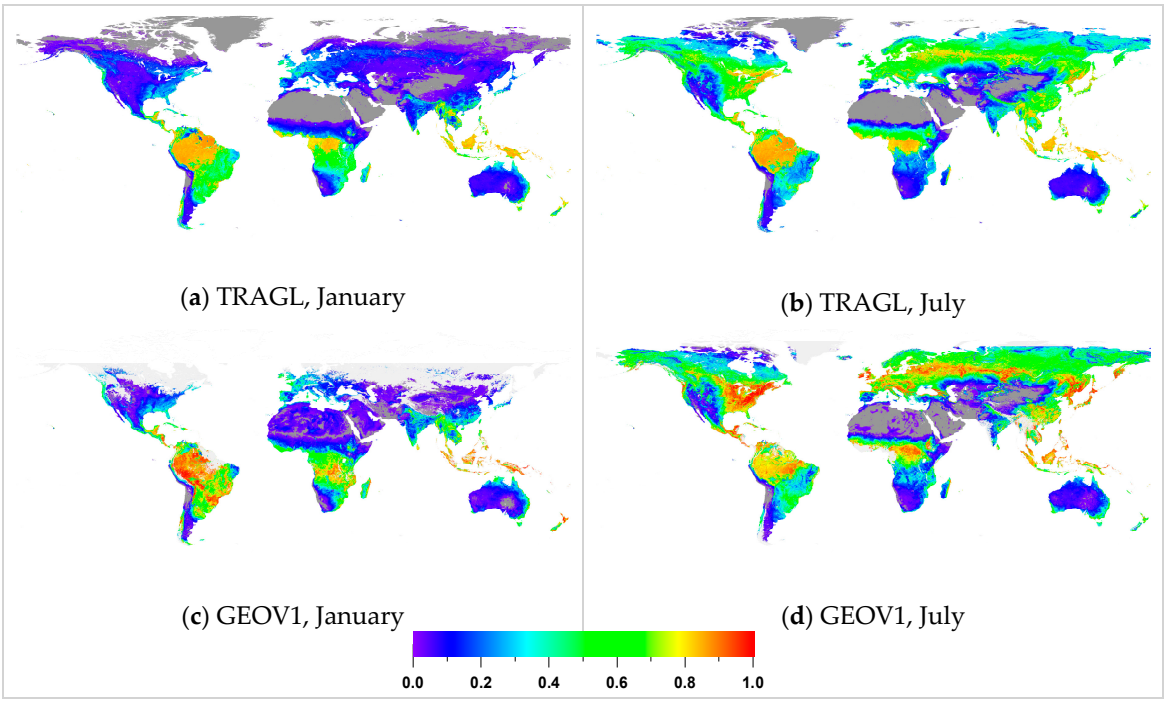

Figure 2. Global mean FCover for TRAGL (**a**,**b**) and GEOV1 (**c**,**d**) products from 2001−2005. **Left panels**: January. **Right panels**: July. Areas masked in dark gray correspond to pixels where the FCover values are zero and areas masked in light gray correspond to pixels where the FCover values are missing.

Statistical distributions of the FCover values for 2001–2005 for each biome type according to the MODIS land cover type are shown in Figure 3 to illustrate the similarities and differences between the TRAGL and GEOV1 FCover products. For grasses and cereal crops, shrubs, evergreen needle forests, and deciduous needle forests, the histogram distributions of the TRAGL FCover values are generally consistent with those of the GEOV1 FCover values. For the savannah biome type, the frequencies of TRAGL FCover values between 0.1 and 0.6 are significantly larger than those of GEOV1 FCover values, while the frequencies of TRAGL FCover values greater than 0.6 are significantly less than those of GEOV1 FCover values and reduce to 0 when FCover values are greater than 0.85. Similar distributions of FCover values are also observed for evergreen broadleaf forests and deciduous broadleaf forests. For the evergreen broadleaf forests, TRAGL and GEOV1 FCover values have distributions with a narrow peak, but the TRAGL frequency distribution peak (approximately 0.8) is slightly lower than that of GEOV1.

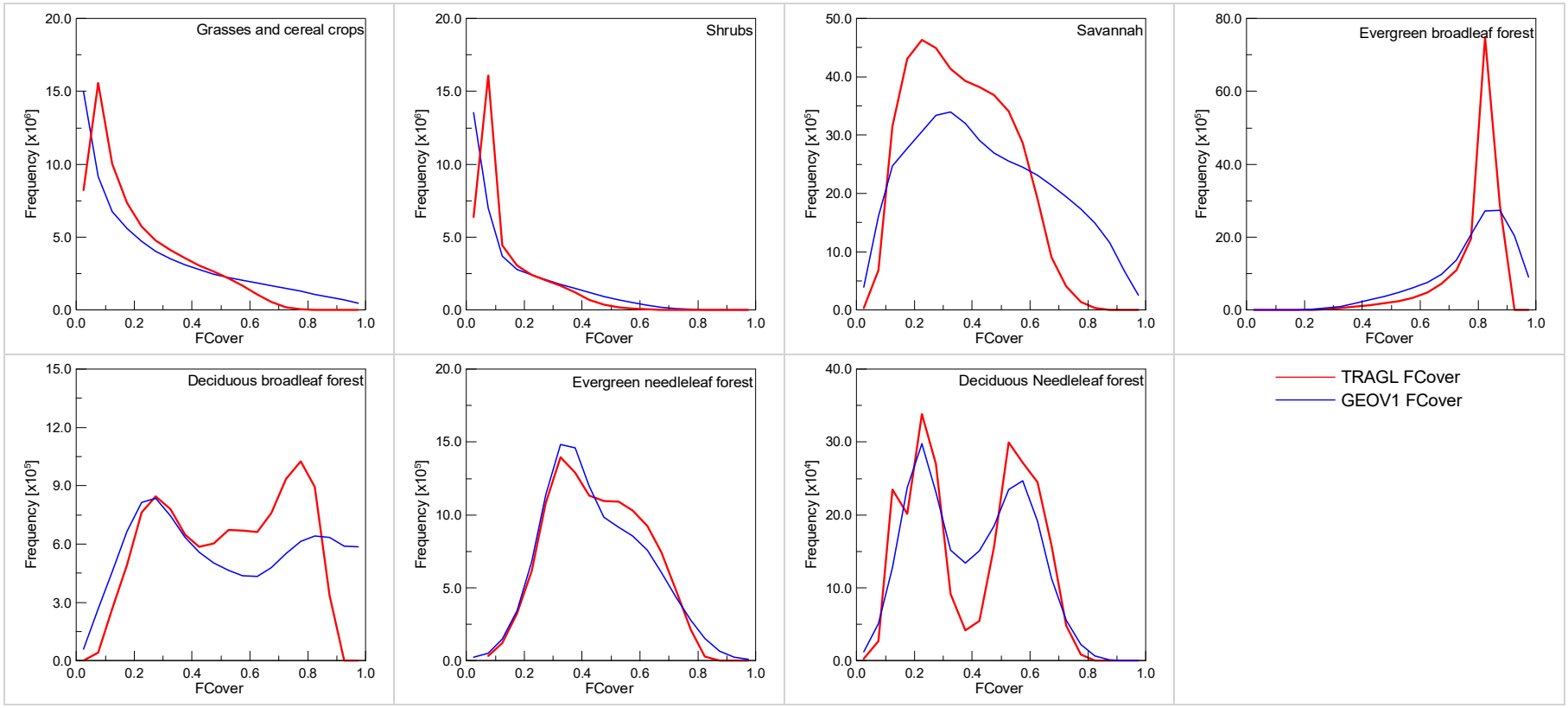

Figure 3. Histograms of the TRAGL and GEOV1 FCover products for 2001–2005 for different biome types.

Figure 4 shows mean values of the FCover differences for different 10°-latitude bands in each month for 2001–2005. In most latitude bands for each month, the mean FCover differences between TRAGL and GEOV1 FCover products are within ±0.05, indicating that the TRAGL FCover values for these regions are in good agreement with the corresponding GEOV1 FCover values. However, there are slight discrepancies between them for low and high latitudes. The TRAGL FCover values were smaller than those of GEOV1 over the 5°N–15°N latitude band from July to October, and the 5°S–15°S latitude band from January to April. The mean values of the FCover differences over these regions reach 0.14. The TRAGL FCover values were also smaller than those of GEOV1 over the 65°N–75°N latitude band, especially in October. However, the TRAGL FCover values were larger than those of GEOV1 over the 55°N–65°N latitude band in February and April and the 65°S–75°S latitude band, especially in May and August.

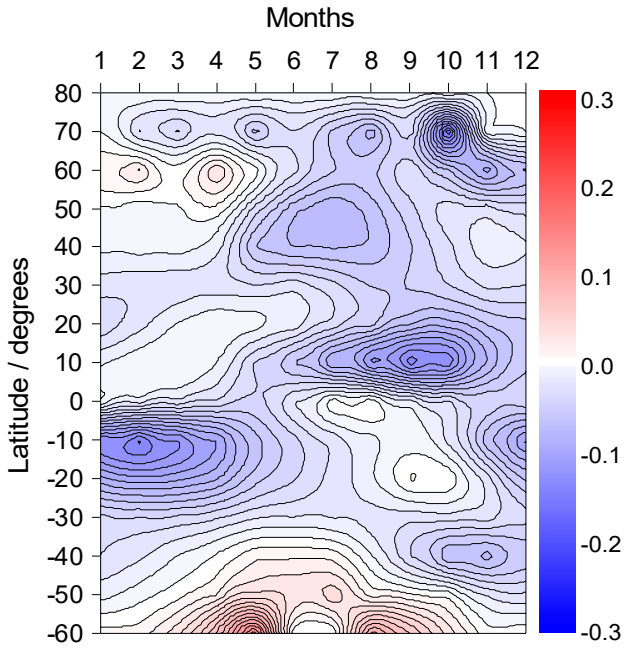

Figure 4. Hovmoller diagram of mean values of the FCover differences between TRAGL and GEOV1 FCover products for different 10°-latitude bands in each month for 2001–2005.

Figure 5 shows mean values of TRAGL and GEOV1 FCover products for different biome types in each month for 2001–2005. The standard deviations and the relative differences [100× | FCoverTRAGL-FCoverGEOV1 | /FCoverTRAGL] for the mean values are also shown in Figure 5. The numbers of pixels to calculate the mean values and standard deviations across different biomes for each month are shown in Table 3. The largest relative differences between TRAGL and GEOV1 FCover products occur for grasses/cereal crops and savannah, where the TRAGL FCover values were always lower than the GEOV1 FCover values in all months. For the grasses/cereal crops, the TRAGL FCover values were between 15% and 35% lower than the GEOV1 FCover values, whereas for the savannah, the TRAGL FCover values were between 20% and 30% lower than the GEOV1 FCover values. For shrubs, there are large differences between the TRAGL and GEOV1 FCover products from April to November, when the relative differences were more than 15% and the TRAGL and GEOV1 FCover values also show the largest standard deviation. There is an excellent agreement between TRAGL and GEOV1 FCover products for evergreen broadleaf forests in all months, with maximum relative differences of only 3.75% in July. The TRAGL and GEOV1 FCover products also show an excellent agreement for evergreen needleleaf forests, where the relative differences are less than 5% for all months except March, November, and December. The largest differences for the

evergreen needleleaf forests are observed in December, when the TRAGL FCover values were 27% lower than the GEOV1 FCover values.

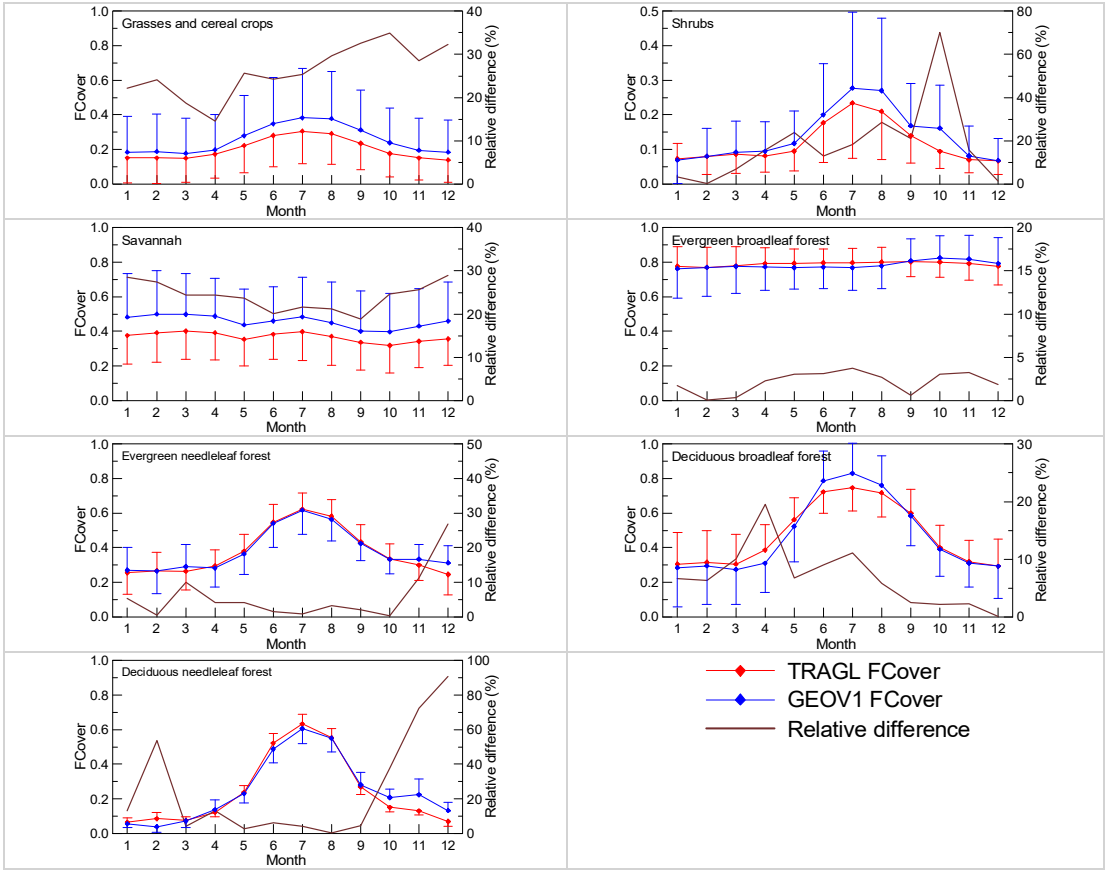

Figure 5. Mean values of TRAGL and GEOV1 FCover products for different biome types in each month for 2001–2005 and their relative differences.

For deciduous broadleaf forest, small differences between the TRAGL and GEOV1 FCover products are observed from January to August, while the TRAGL FCover product achieves good agreement with the GEOV1 FCover product from September to December. The TRAGL FCover values are between 0.05 and 0.1 lower than those of GEOV1 from June to August, but the TRAGL FCover values are slightly higher than those of GEOV1 for the other months. For deciduous needleleaf forests, the TRAGL and GEOV1 FCover products show good consistency in all months except February, October, November, and December. The largest relative difference of 90.75% is observed in December.

For grasses/cereal crops, shrubs and deciduous broadleaf forest, there are large discrepancies between the TRAGL and GEOV1 FCover products during the growing seasons, which may result from the difficulty of acquiring cloud-free images in this time period due to the high humidity in the atmosphere. In addition, there are high relative differences between the TRAGL and GEOV1 FCover products in the spring or winter for some biome types, such as evergreen needleleaf forests and deciduous needleleaf forests, which may partly result from the limited number of pixels to calculate the mean values and standard deviations (Table 3). For instance, there are only 788 pixels for which TRAGL and GEOV1 FCover products provided FCover values in February for the deciduous needleleaf forests. In other words, less than 1% of the pixels in summer contributed to the February values. The main reason for this limited number of pixels is that deciduous needleleaf forests are mainly situated in the higher northern hemisphere and optical remote sensing in February is extremely difficult in high latitudes.

Table 3. The number of pixels to calculate the mean values and standard deviationsacross different biomes for 12 months.

Month	GCC	SHB	SVN	EBF	DBF	ENF	DNF
Jan	985,636	451,663	641,547	372,828	128,491	55,625	4510
Feb	1,025,756	451,616	641,364	357,647	122,924	78,354	788
Mar	1,178,315	455,838	648,645	364,684	153,906	85,715	2804
Apr	1,350,668	458,903	690,889	374,780	231,431	219,956	11,055
May	1,397,863	588,449	895,854	360,526	253,126	325,827	85,608
Jun	1,456,798	1,058,810	946,856	357,754	251,286	336,228	88,049
Jul	1,524,155	1,094,476	930,176	362,374	246,499	339,242	88,050
Aug	1,501,161	1,094,436	904,858	368,948	245,460	337,507	88,050
Sep	1,555,865	1,094,892	942,266	391,350	250,847	340,780	88,050
Oct	1,470,197	866,052	944,379	401,671	253,335	341,358	87,477
Nov	1,383,669	486,386	729,848	380,965	235,894	242,110	21,725
Dec	1,161,229	454,034	654,806	360,736	173,795	87,783	6812

GCC = Grasses and cereal crops; SHB = Shrubs; BLC = Broadleaf crops; SVN = Savannah; EBF = Evergreen broadleaf forests; DBF = Deciduous broadleaf forests; ENF = Evergreen needleleaf forests; DNF = Deciduous needleleaf forests.

4.1.2. Temporal Consistency

Figure 6 shows the temporal FCover profiles to evaluate temporal consistency between the TRAGL and GEOV1 FCover products over several sites with different biome classes. The temporal FCover trajectories for the Zhangbei, Larzac, and Laprida sites with grass and cereal crop biome types are shown in Figure 6a. For the Zhangbei site, the TRAGL FCover values were slightly higher than the GEOV1 FCover values of nearly zero during the non-growing season, but the TRAGL FCover values were slightly smaller than the GEOV1 FCover values during the growing season. The GEOV1 FCover values for days 225, 236, and 358 were missing. The TRAGL FCover values were in agreement with the mean value of the high resolution FCover map. For the Larzac and Laprida sites, the GEOV1 FCover values were higher than those of TRAGL throughout the entire year in 2002. The TRAGL FCover values were slightly overestimated with values of 0.12 compared with the mean value of the high-resolution FCover map at the Larzac site, whereas the TRAGL FCover values became slight underestimates when compared to the mean value of the high resolution FCover map at the Laprida site.

The temporal FCover profiles for the Demmin, Apilles2, and Barrax sites are shown in Figure 6b. The biome type for these sites is broadleaf crops. At these sites, the GEOV1 FCover values were larger than those of TRAGL, especially during the growing season, although some GEOV1 FCover values were missing. At the Demmin site, the GEOV1 FCover displays very high values up to 0.96 for days 155, 165, 175, and 185. However, the TRAGL FCover values demonstrated exceptionally good agreement with the mean values of the high resolution FCover maps. The absolute differences between the TRAGL FCover values and the mean values of the high resolution FCover maps were less than 0.05 at these sites.

The temporal FCover trajectories for broadleaf forest sites are shown in Figure 6c. For the Counami site, most GEOV1 FCover values for 2001 are missing, whereas TRAGL FCover values have continuous trajectory. For the Cameron and Puechabon sites, TRAGL FCover profiles are in good agreement with those of GEOV1 in terms of seasonal patterns and absolute FCover values. For the Counami and Cameron sites, the TRAGL and GEOV1 FCover values are approximately constant for the entire year and present almost no seasonality as expected for these evergreen forests, which is consistent with the findings of Camacho *et al.* [19]. The agreement of the TRAGL FCover values with the mean values of the high-resolution FCover maps is very good with overestimates less than 0.054 at these sites.

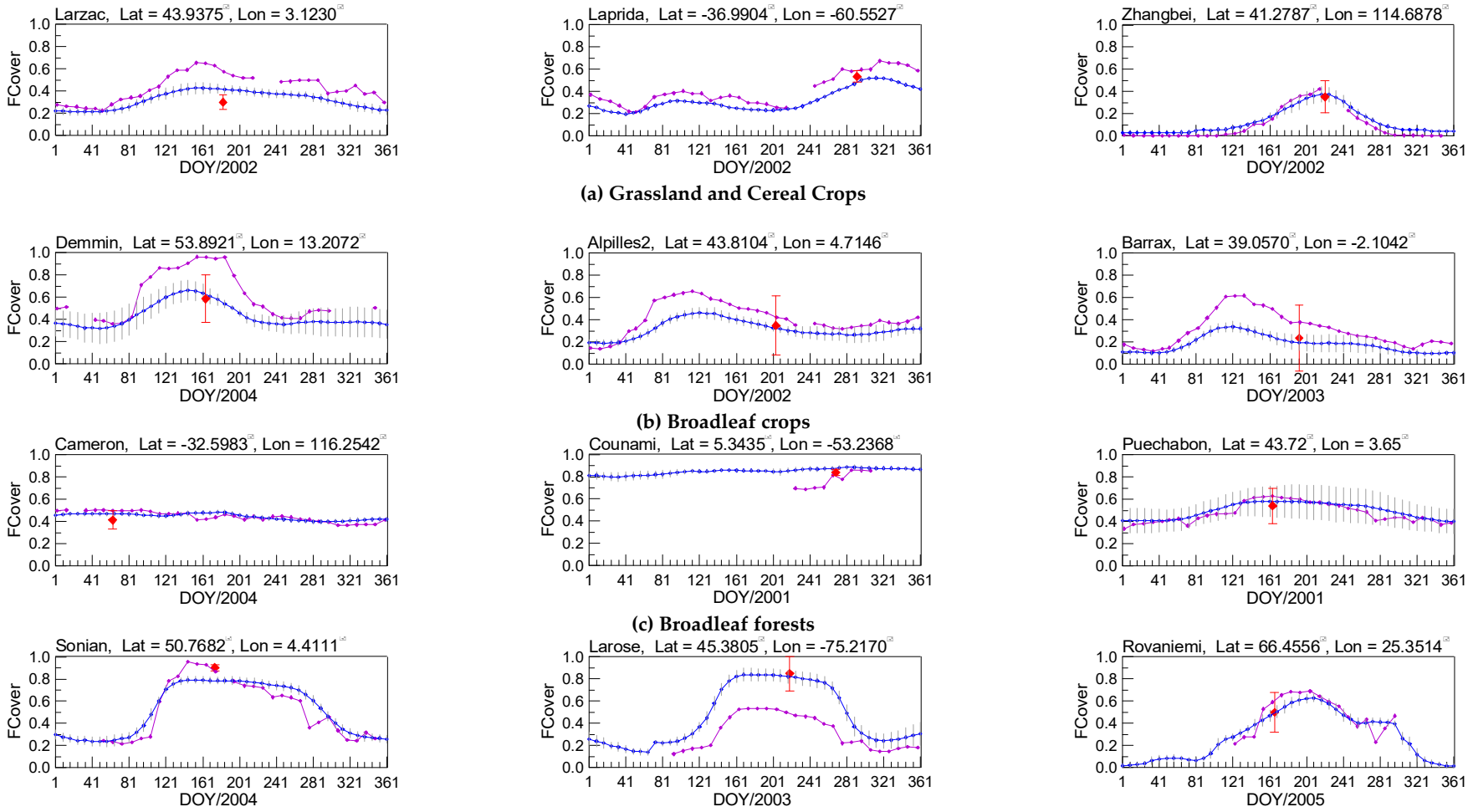

Figure 6. *Cont.*

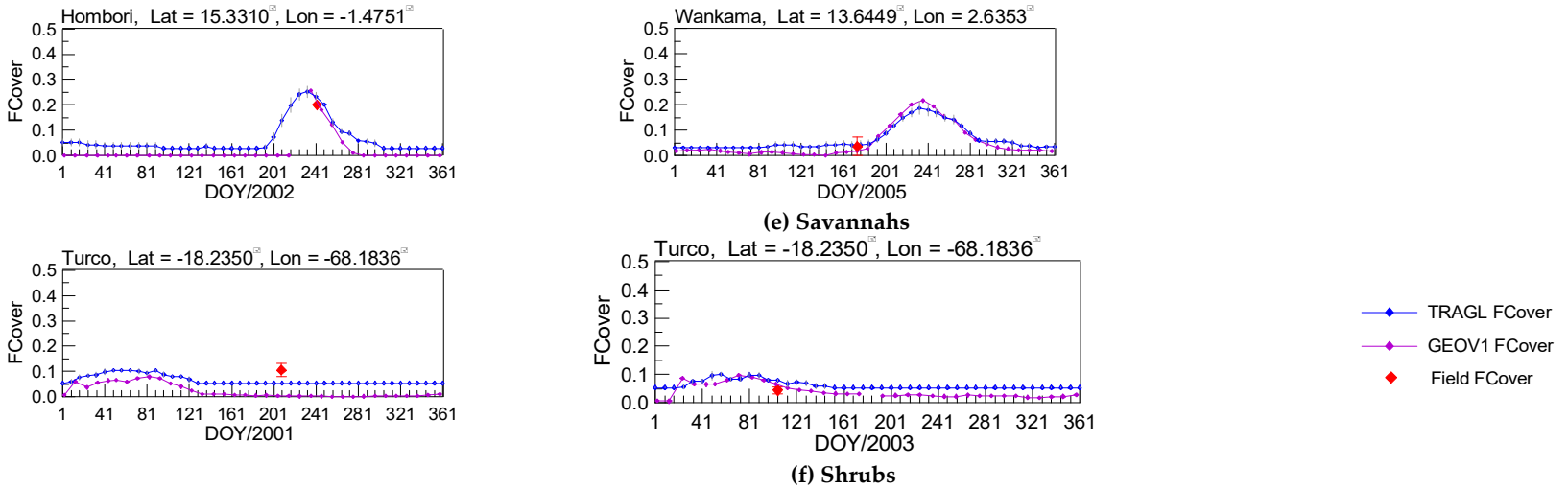

Figure 6. Temporal profiles of the TRAGL and GEOV1 FCover values for several sites with different vegetation types: (**a**) Grassland and Cereal Crops; (**b**) Broadleaf crops; (**c**) Broadleaf forests; (**d**) Needleleaf forests; and (**e**) Savannahs and (**f**) Shrubs.

Figure 6d shows the temporal FCover trajectories for needleleaf forest biome sites. For the Sonian and Rovaniemi site, the temporal FCover trajectories of TRAGL and GEOV1 show good agreement, although some FCover values are missing in the GEOV1 FCover product. However, the TRAGL FCover values are between 0.1 and 0.31 higher than those of GEOV1 at the Larose site. For the Larose and Rovaniemi sites, the TRAGL FCover values demonstrated excellent agreement with the mean values of the high-resolution FCover maps, but at the Sonian site, the TRAGL FCover values were slightly underestimated with values of 0.12 compared with the mean values of the high-resolution FCover maps.

The temporal FCover profiles for the Hombori and Wankama sites with savannah biome type are shown in Figure 6e. There are large discrepancies for the Hombori site. Many GEOV1 FCover values were missing at the beginning of the growing season. During the non-growing season, the GEOV1 FCover values, at nearly zero, are almost 0.05 lower than those of TRAGL. For the Wankama site, the TRAGL FCover values are in generally good agreement with the GEOV1 FCover values, in terms of seasonal patterns. Similarly to the Hombori site, the GEOV1 FCover values are slightly lower than those of TRAGL during the non-growing season. However, the GEOV1 FCover values are slightly higher than those of TRAGL during the growing season.

The temporal FCover trajectories for Turco site with shrub biome type in 2001 and 2003 are shown in Figure 6f. The TRAGL and GEOV1 FCover products show very low values as expected, with little seasonality. The FCover values for both FCover products were less than 0.1 during these years. TRAGL FCover shows slightly higher values than GEOV1 FCover, especially during the non-growing season. At this site, the TRAGL FCover values were slightly underestimated with values of 0.051 in 2001 and slightly overestimated by 0.036 in 2003 when compared to the mean values of the high-resolution FCover maps.

4.2. Direct Validation

Scatterplots of the FCover products versus the mean values of the high-resolution FCover maps are shown in Figure 7. The majority of points in Figure 7b are above the 1:1 line, which indicates that GEOV1 FCover values are higher than the mean values of the high-resolution FCover maps, especially for high FCover values. These overestimation of high FCover values should be partly explained by a slightly too large scaling factor which was applied to scale CYCLOPES FCover values [7]. Compared with GEOV1 FCover values, those of TRAGL are distributed more closely around the 1:1 line against the mean values of the high-resolution FCover maps (Figure 7a), showing that TRAGL FCover product achieves better agreement across the FCover range than the GEOV1 FCover products.

It is apparent that the TRAGL FCover product provides slightly better accuracy against the mean values of the high-resolution FCover maps (RMSE = 0.0865, and bias = 0.0171) compared with the GEOV1 FCover product (RMSE = 0.1541, and bias = 0.0754). The correlation between the TRAGL FCover values and the mean values of the high-resolution FCover maps (R^2 = 0.8848) is also superior to the correlations of the GEOV1 FCover values (R^2 = 0.7621) with the mean values of the high-resolution FCover maps.

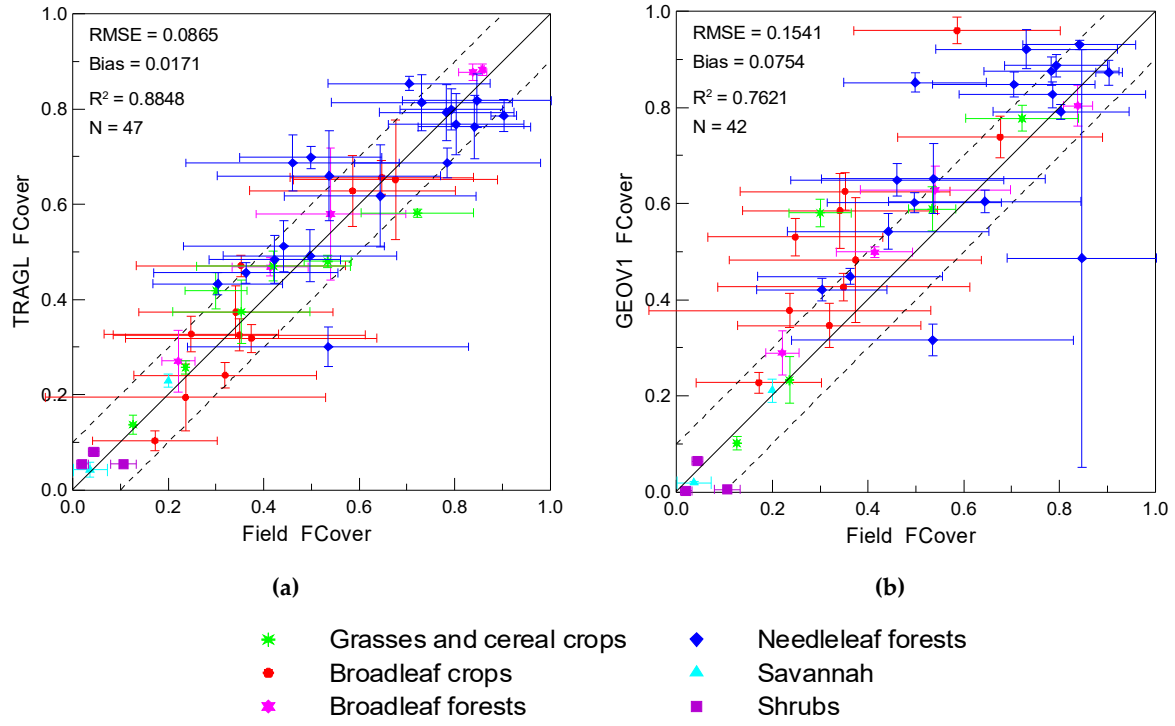

Figure 7. Scatterplots of (**a**) TRAGL and (**b**) GEOV1 FCover products *versus* mean values of the high resolution FCover maps. The R-squared, RMSE, and bias values are also shown. N is the number of matched data pairs for each case.

5. Discussions

The method proposed in this study calculated TRAGL FCover values from the GLASS LAI product to ensure physical consistency between LAI and FCover retrievals. The GLASS LAI retrieval algorithm estimated the LAI annual profile using annual observations. The GRNNs used in GLASS LAI production use the surface reflectance for a one-year period as their input. The output is a one-year LAI profile for each pixel. Extensive validation and analysis demonstrated that the GLASS LAI product is spatially complete and temporally continuous, and the accuracy of GLASS LAI product is better than several existing LAI products. Therefore, the TRAGL FCover product also shows temporally continuous and smooth FCover profiles and better performance as compared to ground-based estimates.

On the downside, the surface-reflectance data for a one-year period were entered into the GRNNs to estimate the one-year LAI profiles. The GLASS LAI retrieval algorithm is essentially a reanalysis method. It is impossible to provide near-real-time retrievals for the GLASS LAI retrieval algorithm. Therefore, the method proposed in this paper also cannot carry out real-time/near real-time estimation of FCover values because of the dependence on the GLASS LAI product.

Additionally, the quality of the GLASS LAI product has a direct impact on the quality of the TRAGL FCover product. The GLASS LAI retrieval algorithm can remove abrupt spikes and dips, which may lead to the loss of neighboring smaller peaks in LAI profiles. Therefore, The TRAGL FCover product also cannot describe more local (in time) impacts of disturbances such as fire, disease, and insect damage.

6. Conclusions

A pragmatic method is proposed to derive physically consistent FCover values from the GLASS LAI product and other ancillary information. The quality and accuracy of the generated FCover

product (TRAGL) were evaluated by comparison with GEOV1 FCover product and directly validated against ground-based FCover estimates.

The TRAGL FCover product is spatially and temporally complete. Comparison with GEOV1 FCover product showed that both FCover products were generally consistent in their spatial patterns. However, there were relatively large discrepancies in the relative magnitude of the FCover products over equatorial rainforests, broadleaf crops in east central United States and needleleaf forests in Europe and Siberia. TRAGL FCover product had continuous trajectories. The temporal profiles of TRAGL and GEOV1 FCover products showed consistent seasonal variations. Direct validation with ground-based FCover estimates showed that TRAGL FCover product provided the better accuracy against the mean values of high-resolution FCover maps compared with the GEOV1 FCover product. The GEOV1 FCover product shows a slight overestimation of the ground-based FCover estimates, particularly for high FCover values.

The proposed method was used to calculate FCover values based on the GLASS LAI data derived from MODIS reflectance data. In the near future, we will extend this method to calculate FCover values based on the GLASS LAI data derived from AVHRR reflectance data and perform more extensive validation and analysis of TRAGL FCover values.

Acknowledgments: This work was financially supported through Grant No. 2013AA121201 under the "State Program for High-Tech Research and Development (863 program)", the Chinese 973 Program under Grant No. 2013CB733403 and the National Natural Science Foundation of China under Grant Nos. 41171264 and 41331173.

Author Contributions: Zhiqiang Xiao and Shunlin Liang conceived the study; Zhiqiang Xiao, Tongtong Wang and Rui Sun performed the data analysis; Zhiqiang Xiao wrote the paper. Shunlin Liang, Tongtong Wang and Rui Sun reviewed and edited the manuscript. All authors read and approved the manuscript.

Conflicts of Interest: The authors declare no conflict of interest.

References

1. Gutman, G.; Ignatov, A. The derivation of the green vegetation fraction from NOAA/AVHRR data for use in numerical weather prediction models. *Int. J. Remote Sens.* **1998**, *19*, 1533–1543. [CrossRef]
2. Zeng, X.B.; Dickinson, R.E.; Walker, A.; Shaikh, M.; DeFries, R.S.; Qi, J. Derivation and evaluation of global 1-km fractional vegetation cover data for land modeling. *J. Appl. Meteorol.* **2000**, *39*, 826–839. [CrossRef]
3. Baret, F.; Hagolle, O.; Geiger, B.; Bicheron, P.; Miras, B.; Huc, M.; Berthelot, B.; Nio, F.; Weiss, M.; Samain, O.; *et al.* LAI, fAPAR and fCover CYCLOPES global products derived from VEGETATION: Part 1: Principles of the algorithm. *Remote Sens. Environ.* **2007**, *110*, 275–286. [CrossRef]
4. Jia, K.; Liang, S.; Liu, S.; Li, Y.; Xiao, Z.; Yao, Y.; Jiang, Bo.; Zhao, X.; Wang, X.; Xu, S.; Cui, J. Global land surface fractional vegetation cover estimation using general regression neural networks from MODIS surface reflectance. *IEEE Trans. Geosci. Remote Sens.* **2015**, *53*, 4787–4796. [CrossRef]
5. Zhang, X.; Liao, C.; Li, J.; Sun, Q. Fractional vegetation cover estimation in arid and semi-arid environments using HJ-1 satellite hyperspectral data. *Int. J. Appl. Earth Observ. Geoinf.* **2013**, *21*, 506–512. [CrossRef]
6. Roujean, J.L.; Lacaze, R. Global mapping of vegetation parameters from POLDER multiangular measurements for studies of surfaceatmosphere interactions: A pragmatic method and its validation. *J. Geophys. Res. Atmos.* **2002**, *107*. [CrossRef]
7. Baret, F.; Weiss, M.; Lacaze, R.; Camacho, F.; Makhmara, H.; Pacholcyzk, P.; Smets, B. GEOV1: LAI and FAPAR essential climate variables and FCOVER global time series capitalizing over existing products. Part 1: Principles of development and production. *Remote Sens. Environ.* **2013**, *137*, 299–309. [CrossRef]
8. Elmore, A.J.; Mustard, J.F.; Manning, S.J.; Lobell, D.B. Quantifying vegetation change in semiarid environments: Precision and accuracy of spectral mixture analysis and the normalized difference vegetation index. *Remote Sens. Environ.* **2000**, *73*, 87–102. [CrossRef]
9. Hurcom, S.J.; Harrison, A.R. The NDVI and spectral decomposition for semi-arid vegetation abundance estimation. *Int. J. Remote Sens.* **1998**, *19*, 3109–3125. [CrossRef]
10. Patel, N.K.; Saxena, R.K.; Shiwalkar, A.J.A.Y. Study of fractional vegetation cover using high spectral resolution data. *J. Indian Soc. Remote Sens.* **2007**, *35*, 73–79. [CrossRef]

11. Gitelson, A.A.; Kaufman, Y.J.; Stark, R.; Rundquist, D. Novel algorithms for remote estimation of vegetation fraction. *Remote Sens. Environ.* **2002**, *80*, 76–87. [CrossRef]
12. Peter, R.J. North Estimation of fAPAR, LAI, and vegetation fractional cover from ATSR-2 imagery. *Remote Sens. Environ.* **2002**, *80*, 114–121.
13. Kenneth, M.G.; Timothy, M.; Lynn, F. Hyperspectral mixture modeling for quantifying sparse vegetation cover in arid environments. *Remote Sens. Environ.* **2000**, *72*, 360–374.
14. Theseira, M.A.; Thomas, G.; Sannier, C.A.D. An evaluation of spectral mixture modeling applied to a semi-arid environment. *Int. J. Remote Sens.* **2002**, *23*, 687–700. [CrossRef]
15. Hobbs, S.E.; Thomas, G. A goodness-of-fit measure applied to spectral mixture modelling. In *Image Processing: Mathematical Methods and Applications*; Blackledge, J., Ed.; Oxford University Press: Oxford, UK, 1996; pp. 317–331.
16. Qi, J.; Marsett, R.C.; Moran, M.S.; Goodrich, D.C.; Heilman, P.; Kerr, Y.H.; Dedieu, G.; Chehbouni, A.; Zhang, X.X. Spatial and temporal dynamics of vegetation in the San Pedro River basin area. *Agric. Forest Meteorol.* **2000**, *105*, 55–68. [CrossRef]
17. Kimes, D.S.; Knyazikhin, Y.; Privette, J.L.; Abuelgasim, A.A.; Gao, F. Inversion methods for physically-based models. *Remote Sens. Rev.* **2000**, *18*, 381–439. [CrossRef]
18. Bacour, C.; Baret, F.; Béal, D.; Weiss, M.; Pavageau, K. Neural network estimation of LAI, fAPAR, fCover and LAI×Cab, from top of canopy MERIS reflectance data: Principles and validation. *Remote Sens. Environ.* **2006**, *105*, 313–325. [CrossRef]
19. Camacho, F.; Cernicharo, J.; Lacaze, R.; Baret, F.; Weiss, M. GEOV1: LAI, FAPAR essential climate variables and FCOVER global time series capitalizing over existing products. Part 2: Validation and intercomparison with reference products. *Remote Sens. Environ.* **2013**, *137*, 310–329. [CrossRef]
20. Xiao, Z.; Liang, S.; Wang, J.; Xie, D.; Song, J.; Fensholt, R. A Framework for Consistent Estimation of Leaf Area Index, Fraction of Absorbed Photosynthetically Active Radiation, and Surface Albedo from MODIS Time-Series Data. *IEEE Trans. Geosci. Remote Sens.* **2015**, *53*, 3178–3197. [CrossRef]
21. Huemmrich, K.F.; Privette, J.L.; Mukelabai, M.; Myneni, R.B.; Knyazikhin, Y. Time-series validation of MODIS land biophysical products in a Kalahari woodland, Africa. *Int. J. Remote Sens.* **2005**, *26*, 4381–4398. [CrossRef]
22. Liang, S.; Zhang, X.; Xiao, Z.; Cheng, J.; Liu, Q.; Zhao, X. *Global LAnd Surface Satellite (GLASS) Products: Algorithms, Validation and Analysis*; Springer: New York, NY, USA, 2013.
23. Liang, S.; Zhao, X.; Yuan, W.; Liu, S.; Cheng, X.; Xiao, Z.; Zhang, X.; Liu, Q.; Cheng, J.; Tang, H.; *et al.* A Long-term Global LAnd Surface Satellite (GLASS) Dataset for Environmental Studies. *Int. J. Digital Earth* **2013**, *6* (Supp. 1), 5–33. [CrossRef]
24. Xiao, Z.; Liang, S.; Wang, J.; Chen, P.; Yin, X.; Zhang, L.; Song, J. Use of general regression neural networks for generating the GLASS leaf area index product from time series MODIS surface reflectance. *IEEE Trans. Geosci. Remote Sens.* **2014**, *52*, 209–223. [CrossRef]
25. Xiao, Z.; Liang, S.; Wang, J.; Xiang, Y.; Zhao, X.; Song, J. Long time-series Global Land Surface Satellite (GLASS) leaf area index product derived from MODIS and AVHRR data. *IEEE Trans. Geosci. Remote Sens.* **2015**, under review.
26. Pedelty, J.; Devadiga, S.; Masuoka, E.; Brown, M.; Pinzon, J.; Tucker, C.; Vermote, E.; Prince, S.; Nagol, J.; Justice, C.; *et al.* Generating a long-term land data record from the AVHRR and MODIS instruments. *IEEE Int. Geosci. Remote Sens. Symp.* **2007**. [CrossRef]
27. The GLASS LAI Product at Beijing Normal University. Available online: http://www.bnu-datacenter.com/en (accessed on 25 November 2015).
28. The GLASS LAI Product at the Global Land Cover Facility. Available online: http://glcf.umd.edu (accessed on 25 November 2015).
29. The Copernicus Land Monitoring Services. Available online: http://land.copernicus.eu/ (accessed on 25 November 2015).
30. The VALERI Validation Data. Available online: http://w3.avignon.inra.fr/valeri/ (accessed on 25 November 2015).
31. Demarez, V.; Duthoit, S.; Weiss, M.; Baret, F.; Dedieu, G. Estimation of leaf area index (LAI) of wheat, maize and sunflower crops using digital hemispherical photographs. *Agric. Forest Meteorol.* **2008**, *148*, 644–655. [CrossRef]

32. Morisette, J.T.; Baret, F.; Privette, J.L.; Myneni, R.B.; Nickeson, J.; Garrigues, S.; Shabanov, N.; Weiss, M.; Fernandes, R.; Leblanc, S.; *et al.* Validation of global moderate-resolution LAI products: A framework proposed within the CEOS Land Product Validation Subgroup. *IEEE Trans. Geosci. Remote Sens.* **2006**, *44*, 1804–1817. [CrossRef]
33. Campbell, S.G.; Norman, J.M. *An Introduction to Environmental Biophysics*, 2nd ed.; Springer-Verlag: New York, NY, USA, 1998.
34. Cukier, R.I.; Fortuin, C.M.; Schuler, K.E.; Petschek, A.G.; Schaibly, J.H. Study of the sensitivity of coupled reaction systems to uncertainties in rate coefficients: I. Theory. *J. Chem. Phys.* **1973**, *59*, 3873–3878. [CrossRef]
35. Cukier, R.I.; Levine, H.B.; Schuler, K.E. Nonlinear sensitivity analysis of multiparameter model systems. *J. Computat. Phys.* **1978**, *26*, 1–42. [CrossRef]
36. Saltelli, A.; Tarantola, S.; Chan, K.P.S. A quantitative model-independent method for global sensitivity analysis of model output. *Technometrics* **1999**, *41*, 39–56. [CrossRef]
37. Saltelli, A. *Sensitivity Analysis in Practice: A Guide to Assessing Scientific Models*; Wiley: Hoboken, NJ, USA, 2004.
38. Ratto, M.; Pagano, A.; Young, P. State dependent parameter metamodelling and sensitivity analysis. *Comput. Phys. Commun.* **2007**, *177*, 863–876. [CrossRef]
39. He, L.; Chen, J.M.; Pisek, J.; Schaaf, C.B.; Strahler, A.H. Global clumping index map derived from the MODIS BRDF product. *Remote Sens. Environ.* **2012**, *119*, 118–130. [CrossRef]